

# The Jastrow antisymmetric geminal power in Hilbert space: theory, benchmarking, and application to a novel transition state

Eric Neuscamman\*

*Department of Chemistry, University of California, Berkeley, California 94720, USA*

(Dated: November 9, 2018)

The Jastrow-modified antisymmetric geminal power (JAGP) ansatz in Hilbert space successfully overcomes two key failings of other pairing theories, namely a lack of inter-pair correlations and a lack of multiple resonance structures, while maintaining a polynomially scaling cost, variational energies, and size consistency. Here we present efficient quantum Monte Carlo algorithms that evaluate and optimize the JAGP energy for a cost that scales as the fifth power of the system size. We demonstrate the JAGP's ability to describe both static and dynamic correlation by applying it to bond stretching in  $\text{H}_2\text{O}$ ,  $\text{C}_2$ , and  $\text{N}_2$  as well as to a novel, multi-reference transition state of ethene. JAGP's accuracy in these systems outperforms even the most sophisticated single-reference methods and approaches that of exponentially-scaling active space methods.

## I. INTRODUCTION

In predicting the effects of correlations between the positions of a molecule's electrons, one must go beyond the independent particle approximation embodied by the Slater determinant ansatz. In most quantum chemical methods used today, correlations are accounted for in an essentially perturbative manner: Kohn-Sham density functional theory [1], Møller-Plesset perturbation theory [2], and single-reference coupled cluster theory [3] all rely on the fundamental assumption that electron correlation does not greatly alter the wave function structure beyond what can be encoded in a single Slater determinant. This assumption can be used to define two classes of electron correlation. Weak, or dynamic, correlations are those that can be incorporated accurately under this essentially perturbative framework. Strong, or static, correlations, on the other hand, are those that cannot be accounted for by perturbing around a single Slater determinant. While this division is certainly not the only useful way to distinguish different classes of electron correlation, it will serve as the definition of weak and strong for the purposes of this manuscript.

Traditionally, the strong electron correlations encountered in excited states, bond dissociations, and transition metal chemistry have been treated using active space theories [4]. Instead of dividing molecular orbitals into occupied and unoccupied categories based on the presence of a large gap in the orbital energy spectrum, which is typically lacking in systems with strong electron correlations, these methods divide orbitals into three categories: low energy orbitals that can be safely assumed to be doubly occupied, high energy orbitals that can be assumed empty, and a set of orbitals near the Fermi energy that admit multiple competitive electronic configurations. While this active space is of course much smaller than the full Hilbert space, it still grows combinatorially

with system size, causing methods that rely on it to scale exponentially.

Here we pursue an alternative approach to electron correlation that does not rely on either the independent particle approximation or the use of an active space. Instead, the conceptual starting point is a molecule whose electrons are organized into a valence bonding pattern constructed from a product of two-electron units (bonds, lone pairs, etc.). This picture is encoded by the perfect pairing (PP) ansatz [5] and its generalizations, in which the wave function is constructed explicitly as an antisymmetric product of two-electron functions (geminals). This approach can be seen as a direct generalization of the Slater determinant, which is product of one-electron functions (orbitals), that seeks to treat electron correlation in a pairwise manner.

There are, however, two major problems with the perfect pairing approach. First, in order to be computationally feasible, additional approximations must be made in which the geminals are constrained to be strongly [5] or at least partially [6] orthogonal to each other, which reduces the ansatz's ability to capture inter-pair electron correlations [7]. Second, the organization of electrons into a single pairing structure makes it difficult to describe wave functions that resonate between multiple valence bonding patterns. This shortcoming causes PP to exhibit sharp cusps in its potential energy surfaces when the energies of solutions corresponding to different pairing motifs cross [8]. Many attempts to repair these problems have been made, including theories based on configuration interaction [9, 10], coupled cluster [8, 11, 12], perturbation theory [10], and Hopf algebra [13, 14]. However, these approaches all violate one or more of PP's important formal properties: size consistency (additive energies of separated subsystems), variational energies, and polynomial cost.

This paper will show that by using the Hilbert space version [15] of the Jastrow-modified antisymmetric geminal power (JAGP) ansatz [16–19], both inter-pair correlations and multiple resonance structures can be described without sacrificing the variational principle, size consistency, or polynomial cost. On its own, the geminal power

---

\*Electronic mail: eric.neuscamman@gmail.com

can create a superposition of multiple resonance structures using non-orthogonal local geminals. However, in addition to the resonance structures we want, this superposition will typically also contain unphysical resonance structures in which too many electrons are present on one bond or atom. By incorporating the Hilbert space Jastrow factor, which can delete terms with undesirable electron concentrations [15], we prune away these unphysical resonance structures to produce the desired superposition of physically relevant valence bond structures, each of which is a product of several non-orthogonal local geminals. We will show that this ansatz captures the most important electron correlations in a variety of strongly correlated molecular examples, and that it can be optimized for a cost that scales polynomially as the fifth power of the system size.

This paper is organized as follows. We begin with an overview of the JAGP ansatz and the variational Monte Carlo (VMC) framework in which our methods are based (Section II A). We then discuss the slightly non-standard way in which we organize the terms of the ab initio Hamiltonian (Section II B) before presenting the polynomial cost algorithms for evaluating (Sections II C and II D) and optimizing (Sections II E and II F) the JAGP energy. We then present results showing the convergence behavior of the optimization (Section III A), performance in a pedagogical example involving  $H_4$  (Section III B), and the accuracy of the method for singlet-state multi-bond stretching (Sections III C and III D), triplet-state multi-bond stretching (Section III E), and barrier height evaluation for a novel ethene hydrogenation mechanism (Section III F). We conclude (Section IV) with a summary of our findings and comments on the future development of the JAGP.

## II. THEORY

### A. Basics

In this paper we work with the JAGP ansatz in Hilbert space, given as

$$|\Psi\rangle = \exp(\hat{J})|\Psi_{\text{AGP}}\rangle \quad (1)$$

$$|\Psi_{\text{AGP}}\rangle = \left( \sum_{r\bar{s}} F_{r\bar{s}} a_r^\dagger a_{\bar{s}}^\dagger \right)^{N/2} |0\rangle \quad (2)$$

$$\hat{J} = \sum_{p \leq q} J_{pq}^{\alpha\alpha} \hat{n}_p \hat{n}_q + \sum_{\bar{p} \leq \bar{q}} J_{\bar{p}\bar{q}}^{\beta\beta} \hat{n}_{\bar{p}} \hat{n}_{\bar{q}} + \sum_{p\bar{q}} J_{p\bar{q}}^{\alpha\beta} \hat{n}_p \hat{n}_{\bar{q}} \quad (3)$$

where  $N/2$  is the number of  $\alpha$  (and  $\beta$ ) electrons,  $\hat{n}_p$  and  $a_p^\dagger$  are the number and creation operators for orbital  $p$ ,  $|0\rangle$  is the vacuum, and other symbols are as defined in Table I. The ‘‘molecular’’ geminal in Eq. (2) may contain a linear combination of any number of the non-orthogonal local geminals that will be involved in different resonance structures, but rather than choosing them by hand we

TABLE I: Notation

$ \mathbf{n}\rangle$	an occupation number vector
$n_o$	number of $\alpha$ orbitals occupied in $ \mathbf{n}\rangle$
$n_u$	number of $\alpha$ orbitals unoccupied in $ \mathbf{n}\rangle$
$n_s$	number of Monte Carlo samples
$p, q, r, s$	indices for general $\alpha$ orbitals
$\bar{p}, \bar{q}, \bar{r}, \bar{s}$	indices for general $\beta$ orbitals
$i, j, k, l$	indices for $\alpha$ orbitals occupied in $ \mathbf{n}\rangle$
$\bar{i}, \bar{j}, \bar{k}, \bar{l}$	indices for $\beta$ orbitals occupied in $ \mathbf{n}\rangle$
$a, b, c, d$	indices for $\alpha$ orbitals unoccupied in $ \mathbf{n}\rangle$
$\bar{a}, \bar{b}, \bar{c}, \bar{d}$	indices for $\beta$ orbitals unoccupied in $ \mathbf{n}\rangle$
$J_{pq}^{\alpha\alpha}$	matrix of $\alpha$ - $\alpha$ Jastrow variables
$J_{\bar{p}\bar{q}}^{\beta\beta}$	matrix of $\beta$ - $\beta$ Jastrow variables
$J_{p\bar{q}}^{\alpha\beta}$	matrix of $\alpha$ - $\beta$ Jastrow variables
$F_{p\bar{q}}$	the full pairing matrix
$\Phi_{i\bar{j}}$	matrix after deleting unoccupied rows and unoccupied columns from $\mathbf{F}$
$R_{a\bar{i}}$	matrix after deleting occupied rows and unoccupied columns from $\mathbf{F}$
$C_{i\bar{a}}$	matrix after deleting unoccupied rows and occupied columns from $\mathbf{F}$
$B_{a\bar{b}}$	matrix after deleting occupied rows and occupied columns from $\mathbf{F}$
$\Theta_{\bar{i}j}$	inverse of the occupied pairing matrix $\Phi$

will allow the variational optimization of the pairing matrix  $\mathbf{F}$  to encode whatever geminal structure is most appropriate. Also, note that the concise parameterization of the Jastrow factor in Eq. (3) is entirely equivalent to that used previously [15] and maintains the ability to encode local particle number projection operators of the form

$$\exp\left(-\xi\left(M - \sum_{p \in W} \hat{n}_p\right)^2\right) \quad (4)$$

where  $\xi$  is the projection strength,  $M$  is the desired local particle number, and  $W$  is the set of orbitals defining the local region. This equivalence ensures that the ansatz will remain size consistent.

To evaluate the energy of the JAGP, we use the variational energy expression

$$E = \frac{\langle \Psi | H | \Psi \rangle}{\langle \Psi | \Psi \rangle} = \sum_{\mathbf{n}} \frac{|\langle \mathbf{n} | \Psi \rangle|^2 \langle \mathbf{n} | H | \Psi \rangle}{\langle \Psi | \Psi \rangle \langle \mathbf{n} | \Psi \rangle}, \quad (5)$$

which may be evaluated by variational Monte Carlo (VMC) [20] by sampling a set of occupations  $\Omega$  from the wave function’s probability distribution  $|\langle \mathbf{n} | \Psi \rangle|^2 / \langle \Psi | \Psi \rangle$ . The energy is then estimated as an average of local en-

ergies,

$$E = \frac{1}{n_s} \sum_{\mathbf{n} \in \Omega} \frac{\langle \mathbf{n} | H | \Psi \rangle}{\langle \mathbf{n} | \Psi \rangle} \equiv \frac{1}{n_s} \sum_{\mathbf{n} \in \Omega} E_L(\mathbf{n}), \quad (6)$$

with  $n_s$  being the number of Monte Carlo samples in  $\Omega$ . These samples are generated by a Metropolis-Hastings walk through Hilbert space, which requires us to evaluate wave function probability ratios between different occupation number vectors. If we use one-electron moves, then in order to correctly accept or reject a proposed move that would transfer an electron from orbital  $i$  to orbital  $a$ , we must evaluate ratios of the type  $\langle \mathbf{n} | a_i^\dagger a_a | \Psi \rangle / \langle \mathbf{n} | \Psi \rangle$ . These ratios are also involved in computing local energies, and so we will assume for now that they can be evaluated efficiently, a claim that will be verified over the course of the next few sections.

## B. Hamiltonian

For our purposes, it is convenient to write the ab initio Hamiltonian as

$$H = \sum_{pq} t_{pq} \left( a_p^\dagger a_q + a_{\bar{p}}^\dagger a_{\bar{q}} \right) + \sum_{pqrs} (pq|rs) \left( \frac{1}{2} a_p^\dagger a_q a_r^\dagger a_s + \frac{1}{2} a_{\bar{p}}^\dagger a_{\bar{q}} a_{\bar{r}}^\dagger a_{\bar{s}} + a_p^\dagger a_q a_r^\dagger a_{\bar{s}} \right), \quad (7)$$

where  $(pq|rs)$  are the usual two-electron coulomb integrals [4] in  $(11|22)$  order and  $t_{pq}$  are modified one-electron integrals. These modified integrals,

$$t_{pq} = h_{pq} - \frac{1}{2} \sum_r (pr|rq), \quad (8)$$

where  $h_{pq}$  are the standard one-electron integrals, are necessary to accommodate the ordering we have chosen for the creation and destruction operators in Eq. (7).

Before considering our particular wave function, notice that the subset of Hamiltonian terms that contain only number and hole operators (i.e.  $\hat{n}_p = a_p^\dagger a_p$  and  $\hat{h}_p = a_p a_p^\dagger$ ) will add a wave-function-independent contribution to the local energy,

$$E_0(\mathbf{n}) = \sum_i t_{ii} + \sum_{\bar{i}} t_{\bar{i}\bar{i}} + \sum_{i\bar{j}} (i\bar{i}|\bar{j}\bar{j}) + \frac{1}{2} \left[ \sum_{ij} (i\bar{i}|jj) + \sum_{ia} (ia|ai) + \sum_{\bar{i}\bar{j}} (\bar{i}\bar{i}|\bar{j}\bar{j}) + \sum_{\bar{i}\bar{a}} (\bar{i}\bar{a}|\bar{a}\bar{i}) \right]. \quad (9)$$

Similarly, the two-electron components of  $H$  that contain one but not two number or hole operators may be converted in to one-electron operators by immediately acting

the number or hole operator on  $\langle \mathbf{n} |$  in the numerator of Eq. (6). The energy contribution of terms of this type can be accounted for through the one-electron expressions we will derive below by using an  $\mathbf{n}$ -specific modification of the one-electron integrals,

$$t_{ia}^{\mathbf{n}} = t_{ia} + \sum_j (ia|jj) + \sum_{\bar{j}} (ia|\bar{j}\bar{j}) + \frac{1}{2} \left[ \sum_b (ib|ba) - \sum_j (ja|ij) \right], \quad (10)$$

$$t_{i\bar{a}}^{\mathbf{n}} = t_{i\bar{a}} + \sum_{\bar{j}} (\bar{i}\bar{a}|\bar{j}\bar{j}) + \sum_j (\bar{i}\bar{a}|jj) + \frac{1}{2} \left[ \sum_{\bar{b}} (\bar{i}\bar{b}|\bar{b}\bar{a}) - \sum_{\bar{j}} (\bar{j}\bar{a}|\bar{i}\bar{j}) \right]. \quad (11)$$

With these modifications, the only Hamiltonian operators that remain to be dealt with are one-electron terms of the type  $a_i^\dagger a_a$  and two-electron terms of the type  $a_i^\dagger a_a a_j^\dagger a_b$ , where  $i \neq j$  and  $a \neq b$ , which will be the focus of the next two sections.

## C. AGP energy

We will first show how the local AGP energy  $\langle \mathbf{n} | H | \Psi_{\text{AGP}} \rangle / \langle \mathbf{n} | \Psi_{\text{AGP}} \rangle$  can be calculated efficiently before showing in the next section how the effects of Jastrow factors may be incorporated by an efficient modification of the one- and two-electron integrals. To begin our treatment of the AGP local energy, we recall that the AGP's coefficient for a given occupation number vector is equal to a determinant of the occupied portion of the pairing matrix [21],

$$\langle \mathbf{n} | \Psi_{\text{AGP}} \rangle = \det(\Phi). \quad (12)$$

Thus ratios of the type  $\langle \mathbf{n} | a_i^\dagger a_a | \Psi_{\text{AGP}} \rangle / \langle \mathbf{n} | \Psi_{\text{AGP}} \rangle$  that arise in computing the one-electron component of the local energy are simply ratios of determinants that differ by one row (i.e. row  $i$  has been replaced by row  $a$  in the numerator's determinant). Such ratios can be efficiently computed without evaluating the determinants themselves by using the ‘‘rank  $m$ ’’ matrix determinant lemma [22], which states that for any invertible  $n \times n$  matrix  $\mathbf{A}$

$$\det(\mathbf{A} + \mathbf{U}\mathbf{V}^\top) = \det(\mathbf{I} + \mathbf{V}^\top \mathbf{A}^{-1} \mathbf{U}) \det(\mathbf{A}) \quad (13)$$

for any  $n \times m$  matrices  $\mathbf{U}$  and  $\mathbf{V}$ , where  $\mathbf{I}$  is the  $m \times m$  identity matrix. To evaluate the ratios we need, we construct  $\mathbf{U}$  and  $\mathbf{V}$  such that they replace row  $i$  in the determinant  $\langle \mathbf{n} | \Psi_{\text{AGP}} \rangle$  with its counterpart in the determinant  $\langle \mathbf{n} | a_i^\dagger a_a | \Psi_{\text{AGP}} \rangle$ . This replacement is executed via the rank 1 update defined by

$$U_{k1} = \delta_{ki} \quad V_{k1} = R_{a\bar{k}} - \Phi_{i\bar{k}} \quad (14)$$

where  $\mathbf{U}$  picks out the row to replace,  $\mathbf{V}$  holds the difference between the new and old rows, and  $\delta_{ki}$  is the Kronecker delta. Using these definitions, Eq. (13) allows us to write the ratio we desire as

$$\begin{aligned} \frac{\langle \mathbf{n} | a_i^\dagger a_a | \Psi_{\text{AGP}} \rangle}{\langle \mathbf{n} | \Psi_{\text{AGP}} \rangle} &= 1 + \sum_{\bar{k}l} (R_{a\bar{k}} - \Phi_{i\bar{k}}) \Theta_{\bar{k}l} \delta_{li} \\ &= (\mathbf{R}\Theta)_{ai} \end{aligned} \quad (15)$$

where the second equality follows because  $\Theta$  is the inverse of  $\Phi$ . Recognizing that the  $\beta\beta$  part of the one-electron energy will lead to an analogous formula involving single column replacements, we see that the one-electron part of the local energy may be evaluated as

$$E_1^{\text{AGP}} = \sum_{ia} t_{ia}^{\mathbf{n}} (\mathbf{R}\Theta)_{ai} + \sum_{\bar{i}\bar{a}} t_{\bar{i}\bar{a}}^{\mathbf{n}} (\Theta\mathbf{C})_{\bar{i}\bar{a}} \quad (16)$$

where  $t_{ia}^{\mathbf{n}}$  and  $t_{\bar{i}\bar{a}}^{\mathbf{n}}$  are as defined in Eqs. (10-11).

Note that we need not perform direct matrix inversion to compute  $\Theta$  at each step in our random walk. Rather, we first compute  $\Theta$  directly for the occupation number vector that initiates the walk, after which we update it using the Sherman-Morrison formula each time we make a move. The cost of this updating procedure for  $\Theta$  scales as  $n_s n_o^2$ , which is less than direct inversion's  $n_s n_o^3$  and much less than the  $n_s n_o^2 n_u^2$  that will be required for the overall energy.

For the two-electron component of the Hamiltonian, we will encounter ratios between determinants whose matrices differ by two rows, two columns, or one row and one column, and so we will employ the rank 2 matrix determinant lemma. For the all- $\alpha$ -spin two-electron part, the energy contribution is

$$\begin{aligned} E_{2\alpha\alpha}^{\text{AGP}} &= \frac{1}{2} \sum_{iajb} (ia|jb) \frac{\langle \mathbf{n} | a_i^\dagger a_a a_j^\dagger a_b | \Psi_{\text{AGP}} \rangle}{\langle \mathbf{n} | \Psi_{\text{AGP}} \rangle} \\ &\equiv \frac{1}{2} \sum_{iajb} (ia|jb) \mathcal{R}_{ij}^{ab} \end{aligned} \quad (17)$$

where  $\mathcal{R}_{ij}^{ab}$  is a ratio in which the numerator determinant  $\langle \mathbf{n} | a_i^\dagger a_a a_j^\dagger a_b | \Psi_{\text{AGP}} \rangle$  has substituted rows  $a$  and  $b$  for rows  $i$  and  $j$  relative to  $\langle \mathbf{n} | \Psi_{\text{AGP}} \rangle$ . This double row substitution can be written using the rank 2 update

$$\begin{aligned} U_{k1} &= \delta_{ki} & V_{\bar{k}1} &= R_{a\bar{k}} - \Phi_{i\bar{k}} \\ U_{k2} &= \delta_{kj} & V_{\bar{k}2} &= R_{b\bar{k}} - \Phi_{j\bar{k}} \end{aligned} \quad (18)$$

which when used with Eq. (13) allows us to write the ratios from Eq. (17) as  $2 \times 2$  determinants,

$$\mathcal{R}_{ij}^{ab} = \begin{vmatrix} (\mathbf{R}\Theta)_{ai} & (\mathbf{R}\Theta)_{aj} \\ (\mathbf{R}\Theta)_{bi} & (\mathbf{R}\Theta)_{bj} \end{vmatrix}. \quad (19)$$

We expand this determinant to form the final expression for the AGP's all- $\alpha$ -spin contribution to the two-electron

energy,

$$E_{2\alpha\alpha}^{\text{AGP}} = \frac{1}{2} \sum_{iajb} (ia|jb) \left[ (\mathbf{R}\Theta)_{ai} (\mathbf{R}\Theta)_{bj} - (\mathbf{R}\Theta)_{aj} (\mathbf{R}\Theta)_{bi} \right]. \quad (20)$$

The expression for the all- $\beta$ -spin component is derived analogously via column replacements, resulting in

$$E_{2\beta\beta}^{\text{AGP}} = \frac{1}{2} \sum_{\bar{i}\bar{a}\bar{j}\bar{b}} (\bar{i}\bar{a}|\bar{j}\bar{b}) \left[ (\Theta\mathbf{C})_{\bar{i}\bar{a}} (\Theta\mathbf{C})_{\bar{j}\bar{b}} - (\Theta\mathbf{C})_{\bar{j}\bar{a}} (\Theta\mathbf{C})_{\bar{i}\bar{b}} \right]. \quad (21)$$

Finally, the  $\alpha\beta$  two-electron contribution,

$$E_{2\alpha\beta}^{\text{AGP}} = \sum_{ia\bar{j}\bar{b}} (ia|\bar{j}\bar{b}) \frac{\langle \mathbf{n} | a_i^\dagger a_a a_{\bar{j}}^\dagger a_{\bar{b}} | \Psi_{\text{AGP}} \rangle}{\langle \mathbf{n} | \Psi_{\text{AGP}} \rangle} \quad (22)$$

involves ratios in which row  $i$  is replaced with row  $a$  and column  $\bar{j}$  is replaced with column  $\bar{b}$ . This slightly more complicated case can be dealt with via the rank 2 update

$$\begin{aligned} U_{k1} &= \delta_{ki} & V_{\bar{k}1} &= (1 - \delta_{\bar{k}\bar{j}}) R_{a\bar{k}} + \delta_{\bar{k}\bar{j}} B_{a\bar{b}} - \Phi_{i\bar{k}} \\ V_{\bar{k}2} &= \delta_{\bar{k}\bar{j}} & U_{k2} &= (C_{k\bar{b}} - \Phi_{k\bar{j}}) (1 - \delta_{ki}) \end{aligned} \quad (23)$$

where we have taken care that the element where the row and column cross is handled correctly. This rank 2 update allows us to use the matrix determinant lemma to write (after some algebra similar to but messier than the development in Eqs. (18-20)) the  $\alpha\beta$  two-electron contribution as

$$E_{2\alpha\beta}^{\text{AGP}} = \sum_{ia\bar{j}\bar{b}} (ia|\bar{j}\bar{b}) \left[ (\mathbf{R}\Theta)_{ai} (\Theta\mathbf{C})_{\bar{j}\bar{b}} + \Theta_{\bar{j}i} (\mathbf{B} - \mathbf{R}\Theta\mathbf{C})_{a\bar{b}} \right]. \quad (24)$$

Thus, by repeated use of the matrix determinant lemma, we are able to write the bare AGP's local energy as a sum of the contributions in Eqs. (9), (16), (20), (21), and (24), each of which consists of efficient contractions of the one- and two-electron integrals with different subsections of the pairing matrix  $\mathbf{F}$  and the inverse  $\Theta$  of its occupied part. An inspection of these contributions reveals that the overall cost to compute the AGP's energy in this way scales polynomially as  $n_s n_o^2 n_u^2$ . In the next section, we will show that this scaling remains unchanged upon adding the Jastrow factor.

#### D. Jastrow AGP energy

Having constructed an efficient energy evaluation for the AGP wave function, it remains to add the effects of the Jastrow factor, with which the local energy expres-

sion becomes

$$E_L(\mathbf{n}) = \frac{\langle \mathbf{n} | H \exp(\hat{J}) | \Psi_{\text{AGP}} \rangle}{\langle \mathbf{n} | \exp(\hat{J}) | \Psi_{\text{AGP}} \rangle}. \quad (25)$$

As before, we will begin by handling the one-electron components of  $H$ , after which an analogous but slightly more intricate approach will be developed for the two-electron components.

In incorporating effects of the Jastrow factor on the all-spin one-electron terms of the local energy,

$$E_{1\alpha}^{\text{JAGP}} = \sum_{ia} t_{ia}^{\mathbf{n}} \frac{\langle \mathbf{n} | a_i^\dagger a_a \exp(\hat{J}) | \Psi_{\text{AGP}} \rangle}{\langle \mathbf{n} | \exp(\hat{J}) | \Psi_{\text{AGP}} \rangle}, \quad (26)$$

we will again need to evaluate ratios between wave function coefficients for occupation number vectors differing by one orbital. These ratios are no longer simply the ratios of determinants, but we may still take advantage of the determinantal properties used in the previous section by first converting the Jastrow factors into scalars. To see how this is done, consider the denominator. By acting the Jastrow factor  $\exp(\hat{J})$  to the left, we may convert the number operators  $\hat{n}_p$  and  $\hat{n}_{\bar{p}}$  inside it into the occupation numbers  $n_p$  and  $n_{\bar{p}}$  of  $\langle \mathbf{n} |$ . At this point, the whole Jastrow factor becomes a scalar, which we will write as  $\exp(J(\mathbf{n}))$ , and can be factored out of the expectation value. Doing the same for the numerator and defining  $\mathbf{n}_i^a$  as the result of replacing orbital  $i$  with orbital  $a$  in  $\mathbf{n}$ , the ratio in Eq. (26) becomes the product of a ratio of Jastrow factors and the determinantal ratio we encountered in the previous section,

$$E_{1\alpha}^{\text{JAGP}} = \sum_{ia} t_{ia}^{\mathbf{n}} \frac{\exp(J(\mathbf{n}_i^a))}{\exp(J(\mathbf{n}))} \frac{\langle \mathbf{n} | a_i^\dagger a_a | \Psi_{\text{AGP}} \rangle}{\langle \mathbf{n} | \Psi_{\text{AGP}} \rangle}. \quad (27)$$

We can now simplify the ratio of Jastrows by recognizing that all components of the numerator and denominator Jastrows cancel out except those that touch orbitals  $i$  or  $a$ . Defining the ( $\mathbf{n}$ -dependent) intermediates

$$K_p^\alpha = J_{pp}^{\alpha\alpha} + \sum_{k \neq p} J_{pk}^{\alpha\alpha} + \sum_{\bar{k}} J_{p\bar{k}}^{\alpha\beta} \quad (28)$$

and the Jastrow-transformed one-electron integrals

$$\begin{aligned} \tilde{t}_{ia}^{\mathbf{n}} &= t_{ia}^{\mathbf{n}} \exp(J(\mathbf{n}_i^a) - J(\mathbf{n})) \\ &= t_{ia}^{\mathbf{n}} \exp(K_a^\alpha - K_i^\alpha - J_{ia}^{\alpha\alpha}) \end{aligned} \quad (29)$$

we may rewrite our energy expression as

$$E_{1\alpha}^{\text{JAGP}} = \sum_{ia} \tilde{t}_{ia}^{\mathbf{n}} \frac{\langle \mathbf{n} | a_i^\dagger a_a | \Psi_{\text{AGP}} \rangle}{\langle \mathbf{n} | \Psi_{\text{AGP}} \rangle} = \sum_{ia} \tilde{t}_{ia}^{\mathbf{n}} (\mathbf{R}\Theta)_{ai} \quad (30)$$

where the second equality follows from Eq. (15).

Using the same strategy, we can modify the two electron integrals to account for the Jastrow factor's effect on

the two-electron component of the local energy. The all- $\alpha$  two-electron contribution can be computed by replacing  $(ia|jb)$  in Eq. (20) with the transformed integrals

$$\begin{aligned} [ia|jb] &\equiv (ia|jb) \exp(J(\mathbf{n}_{ij}^{ab}) - J(\mathbf{n})) \\ &= (ia|jb) \exp \left[ \begin{aligned} &K_a^\alpha + K_b^\alpha - K_i^\alpha - K_j^\alpha \\ &+ J_{ab}^{\alpha\alpha} - J_{ia}^{\alpha\alpha} - J_{jb}^{\alpha\alpha} \\ &+ J_{ij}^{\alpha\alpha} - J_{ib}^{\alpha\alpha} - J_{ja}^{\alpha\alpha} \end{aligned} \right], \end{aligned} \quad (31)$$

while the all- $\beta$  contribution is computed using the analogous replacement in Eq. (21). Similarly, the  $\alpha\beta$  component may be evaluated by replacing  $(ia|\bar{j}\bar{b})$  in Eq. (24) with the transformed integrals

$$\begin{aligned} [ia|\bar{j}\bar{b}] &\equiv (ia|\bar{j}\bar{b}) \exp(J(\mathbf{n}_{i\bar{j}}^{a\bar{b}}) - J(\mathbf{n})) \\ &= (ia|\bar{j}\bar{b}) \exp \left[ \begin{aligned} &K_a^\alpha + K_{\bar{b}}^\beta - K_i^\alpha - K_{\bar{j}}^\beta \\ &+ J_{a\bar{b}}^{\alpha\beta} - J_{ia}^{\alpha\alpha} - J_{\bar{j}\bar{b}}^{\beta\beta} \\ &+ J_{i\bar{j}}^{\alpha\beta} - J_{i\bar{b}}^{\alpha\beta} - J_{a\bar{j}}^{\alpha\beta} \end{aligned} \right]. \end{aligned} \quad (32)$$

Putting all these developments together, we see that the JAGP local energy is

$$\begin{aligned} E_L(\mathbf{n}) &= E_0(\mathbf{n}) + \sum_{ia} \tilde{t}_{ia}^{\mathbf{n}} (\mathbf{R}\Theta)_{ai} + \sum_{\bar{i}\bar{a}} \tilde{t}_{\bar{i}\bar{a}}^{\mathbf{n}} (\Theta\mathbf{C})_{\bar{i}\bar{a}} \\ &+ \frac{1}{2} \sum_{iajb} [ia|jb] \left[ (\mathbf{R}\Theta)_{ai} (\mathbf{R}\Theta)_{bj} - (\mathbf{R}\Theta)_{aj} (\mathbf{R}\Theta)_{bi} \right] \\ &+ \frac{1}{2} \sum_{\bar{i}\bar{a}\bar{j}\bar{b}} [\bar{i}\bar{a}|\bar{j}\bar{b}] \left[ (\Theta\mathbf{C})_{\bar{i}\bar{a}} (\Theta\mathbf{C})_{\bar{j}\bar{b}} - (\Theta\mathbf{C})_{\bar{j}\bar{a}} (\Theta\mathbf{C})_{\bar{i}\bar{b}} \right] \\ &+ \sum_{ia\bar{j}\bar{b}} [ia|\bar{j}\bar{b}] \left[ (\mathbf{R}\Theta)_{ai} (\Theta\mathbf{C})_{\bar{j}\bar{b}} + \Theta_{\bar{j}i} (\mathbf{B} - \mathbf{R}\Theta\mathbf{C})_{a\bar{b}} \right], \end{aligned} \quad (33)$$

and that the total energy of Eq. (6) can be evaluated for a cost that scales as  $n_s n_\sigma^2 n_u^2$ . Thus with  $n_s$  growing linearly with system size to control statistical uncertainties, the cost to evaluate the JAGP energy grows polynomially as the fifth power of system size.

## E. Derivative ratios

Before discussing the variational minimization of the JAGP energy, we first lay the groundwork by developing efficient evaluations of terms that we call derivative ratios, which will make the optimization relatively simple to describe. Using the compact derivative notation  $|\Psi^x\rangle \equiv \partial|\Psi\rangle/\partial\mu_x$ , where  $\mu_x$  is the  $x$ th wave function

parameter, we first consider the ‘‘bare’’ derivative ratio

$$\mathcal{D}_{\mathbf{n}}(\mu_x) \equiv \frac{\langle \mathbf{n} | \Psi^x \rangle}{\langle \mathbf{n} | \Psi \rangle}. \quad (34)$$

For Jastrow variables, these ratios are quite trivial,

$$\mathcal{D}_{\mathbf{n}}(J_{pq}^{\alpha\alpha}) = n_p n_q \quad (35)$$

$$\mathcal{D}_{\mathbf{n}}(J_{\bar{p}\bar{q}}^{\beta\beta}) = n_{\bar{p}} n_{\bar{q}} \quad (36)$$

$$\mathcal{D}_{\mathbf{n}}(J_{p\bar{q}}^{\alpha\beta}) = n_p n_{\bar{q}} \quad (37)$$

as a derivative of the exponential in Eq. (1) simply brings down the pair of number operators associated with the Jastrow variable in question. For pairing matrix variables, we see from Eq. (12) that only derivatives with respect to the occupied portion  $\Phi$  will be non-zero and that these may be evaluated via the properties of determinant derivatives,

$$\mathcal{D}_{\mathbf{n}}(\Phi_{i\bar{j}}) = \frac{1}{\det(\Phi)} \frac{\partial \det(\Phi)}{\partial \Phi_{i\bar{j}}} = \Theta_{\bar{j}i}. \quad (38)$$

In addition to the bare derivative ratios, we also define the energy derivative ratios,

$$\mathcal{G}_{\mathbf{n}}(\mu_x) \equiv \frac{\langle \mathbf{n} | H | \Psi^x \rangle}{\langle \mathbf{n} | \Psi \rangle}, \quad (39)$$

which are related to derivatives of the local energy by

$$\mathcal{G}_{\mathbf{n}}(\mu_x) = \frac{\partial E_L(\mathbf{n})}{\partial \mu_x} + \mathcal{D}_{\mathbf{n}}(\mu_x) E_L(\mathbf{n}). \quad (40)$$

We now assert that for a given  $\mathbf{n}$ , the full set of energy derivative ratios can be evaluated analytically at a cost that scales as  $n_o^2 n_u^2$ . To see how, consider that the local energy given in Eq. (33) can be constructed from  $\mathbf{F}$ ,  $\mathbf{J}^{\alpha\alpha}$ ,  $\mathbf{J}^{\beta\beta}$ ,  $\mathbf{J}^{\alpha\beta}$ , and  $\Theta$  using only addition, multiplication, and exponentiation. Furthermore, derivatives of  $\Theta = \Phi^{-1}$  with respect to the elements of  $\Phi$  may be evaluated using the properties of the matrix inverse,

$$\frac{\partial \Theta_{\bar{j}i}}{\partial \Phi_{k\bar{l}}} = -\Theta_{\bar{j}k} \Theta_{\bar{l}i}. \quad (41)$$

Thus the local energy  $E_L(\mathbf{n})$  is a single-output, continuously differentiable function of the inputs  $\mathbf{F}$ ,  $\mathbf{J}^{\alpha\alpha}$ ,  $\mathbf{J}^{\beta\beta}$ , and  $\mathbf{J}^{\alpha\beta}$ , and so by the theory of algorithmic differentiation [23], all of its analytic derivatives with respect to these inputs can be computed for an overall cost that is a small constant multiple of the cost of evaluating  $E_L(\mathbf{n})$  itself. We therefore see that the full set of local energy derivatives, and, by Eq. (40), energy derivative ratios, can be evaluated at a cost that scales as  $n_s n_o^2 n_u^2$ . Although we will omit the detailed equations for  $\mathcal{G}_{\mathbf{n}}(\mu_x)$  here, they can be derived by a straightforward application of adjoint algorithmic differentiation [23] to Eq. (33).

## F. Optimization

We variationally optimize the energy of the JAGP wave function using the linear method (LM) [24, 25], which we will briefly review here. The LM works by repeatedly solving the Schrödinger equation in a special subspace of the full Hilbert space defined by the span of the wave function and its first derivatives. More precisely, we construct the generalized eigenvalue problem

$$\sum_{y \in \{0,1,\dots\}} \langle \Psi^x | H | \Psi^y \rangle c_y = \lambda \sum_{y \in \{0,1,\dots\}} \langle \Psi^x | \Psi^y \rangle c_y \quad (42)$$

where  $|\Psi^x\rangle$  and  $|\Psi^y\rangle$  are shorthand for the derivatives of  $|\Psi\rangle$  with respect to the  $x$ th and  $y$ th wave function parameters  $\mu_x$  and  $\mu_y$ , respectively, and  $|\Psi^0\rangle \equiv |\Psi\rangle$ . After solving this eigenvalue problem for  $\mathbf{c}$ , one updates the parameters by

$$\mu_x \leftarrow \mu_x + c_x / c_0 \quad x \in \{1, 2, \dots\}, \quad (43)$$

after which the updated  $|\Psi\rangle$  will be a good approximation for the subspace eigenfunction defined by  $\mathbf{c}$  so long as the updates  $c_x / c_0$  are not too large.

In order to perform the LM optimization, we must solve Eq. (42), which requires building or at least multiplying by the Hamiltonian and overlap matrices. To see how either of these operations may be accomplished using the derivative ratios presented in the previous section, we insert resolutions of the identity  $\sum_{\mathbf{n}} |\mathbf{n}\rangle \langle \mathbf{n}|$  on both sides, divide by  $\langle \Psi | \Psi \rangle$ , and multiply and divide by the square of the local wave function coefficient  $|\langle \mathbf{n} | \Psi \rangle|^2$  to obtain

$$\begin{aligned} & \sum_{\mathbf{n}} \sum_{y \in \{0,1,\dots\}} \frac{|\langle \mathbf{n} | \Psi \rangle|^2 \langle \Psi^x | \mathbf{n} \rangle \langle \mathbf{n} | H | \Psi^y \rangle}{\langle \Psi | \Psi \rangle \langle \Psi | \mathbf{n} \rangle \langle \mathbf{n} | \Psi \rangle} c_y \\ &= \lambda \sum_{\mathbf{n}} \sum_{y \in \{0,1,\dots\}} \frac{|\langle \mathbf{n} | \Psi \rangle|^2 \langle \Psi^x | \mathbf{n} \rangle \langle \mathbf{n} | \Psi^y \rangle}{\langle \Psi | \Psi \rangle \langle \Psi | \mathbf{n} \rangle \langle \mathbf{n} | \Psi \rangle} c_y \end{aligned} \quad (44)$$

which can be approximated on the Monte Carlo sample set  $\Omega$  as

$$\begin{aligned} & \sum_{\mathbf{n} \in \Omega} \sum_{y \in \{0,1,\dots\}} \frac{\langle \Psi^x | \mathbf{n} \rangle \langle \mathbf{n} | H | \Psi^y \rangle}{\langle \Psi | \mathbf{n} \rangle \langle \mathbf{n} | \Psi \rangle} c_y \\ &= \lambda \sum_{\mathbf{n} \in \Omega} \sum_{y \in \{0,1,\dots\}} \frac{\langle \Psi^x | \mathbf{n} \rangle \langle \mathbf{n} | \Psi^y \rangle}{\langle \Psi | \mathbf{n} \rangle \langle \mathbf{n} | \Psi \rangle} c_y. \end{aligned} \quad (45)$$

Inspecting Eq. (45) makes clear that the Monte Carlo approximations to the Hamiltonian and overlap matrices in the first derivative subspace can either be multiplied by or built explicitly using only the derivative ratios  $\mathcal{D}_{\mathbf{n}}(\mu_x)$  and  $\mathcal{G}_{\mathbf{n}}(\mu_x)$  from Eqs. (34) and (39), and so we see that the LM can therefore be applied efficiently by evaluating these ratios as outlined in the previous section.

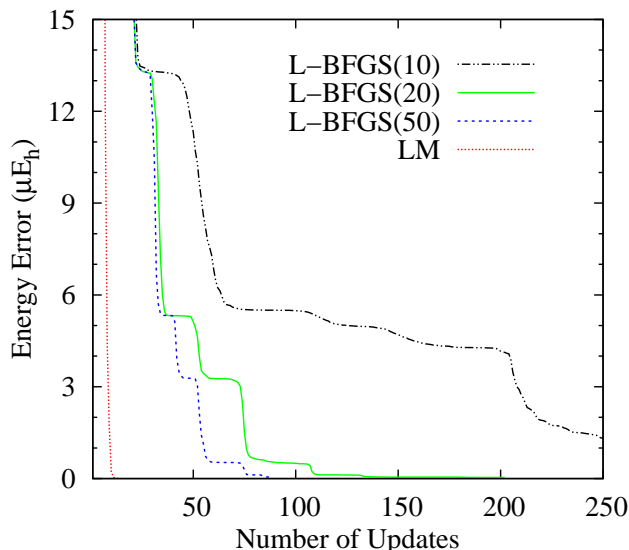


FIG. 1: Convergence of the JAGP energy error vs FCI for two nearby  $H_2$  molecules in the STO-3G basis for different optimization methods, with the numbers in parentheses being the L-BFGS history lengths.

### III. RESULTS

Before we present our results, let us briefly overview the computational details. JAGP calculations used one- and two-electron integrals generated by Psi3 [26], with the atomic orbital basis orthonormalized via the  $S^{-1/2}$  Lowdin procedure. For all methods, we have frozen the 1s core orbital in non-hydrogen elements. Data for full configuration interaction (FCI) [27, 28], complete active space perturbation theory (CASPT2) [29], Davidson-corrected multi-reference configuration interaction (MRCI+Q) [30, 31], and restricted open shell (ROHF) methods were computed using MOLPRO [32]. Data for second order Møller-Plesset perturbation theory (MP2 and UMP2) [2], unrestricted perfect pairing (UPP) [33], B3LYP [34], and coupled cluster with singles, doubles, and perturbative triples (CCSD(T) and UCCSD(T)) [3] were computed using QChem [35].

#### A. Convergence of linear method

We begin our results by looking at two examples illustrating the convergence properties of the linear method optimization. In the first example, we perform an energy optimization on two neighboring  $H_2$  molecules (with atom xyz positions in Angstroms [0.0, 0.0, 0.0], [1.0, 0.0, 0.0], [0.2, 3.0, -0.1], and [0.2, 3.0, 0.9]) in a minimal STO-3G basis [36]. To remove any confusion caused by statistical uncertainty in Monte Carlo sampling, we have executed the optimizations for this example on an “exact” sample, in which every occupation number vector is visited once and given a weight of  $|\langle \mathbf{n} | \Psi \rangle|^2$ . Thus here

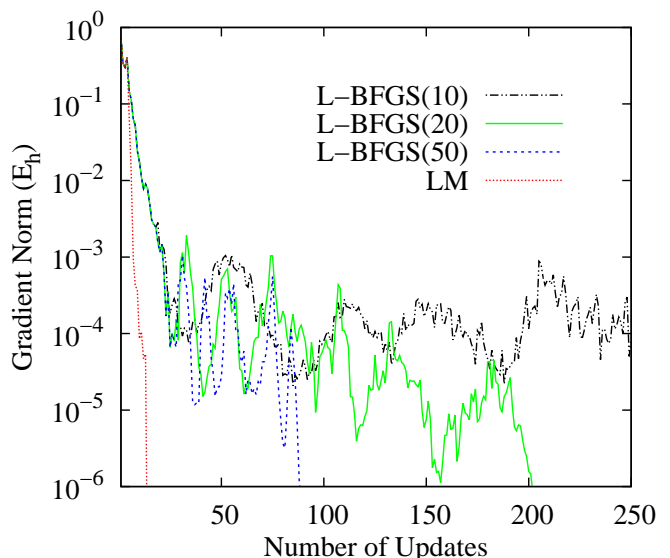


FIG. 2: Convergence of the JAGP energy gradient for two nearby  $H_2$  molecules in the STO-3G basis for different optimization methods, with the numbers in parentheses being the L-BFGS history lengths.

we are concerned only with the quality of the LM optimization in an ideal case. The next example will show concerns that arise during normal Monte Carlo sampling.

In this first example we compare the effectiveness of the LM with that of the low-memory BFGS algorithm (L-BFGS) [37], which performs a quasi-Newton minimiza-

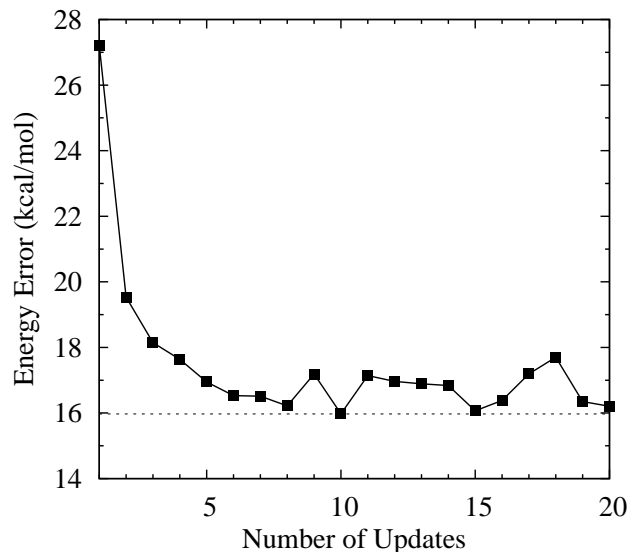


FIG. 3: Convergence of the JAGP energy error vs FCI for  $N_2$  at  $r_{NN} = 1.4 \text{ \AA}$  in the 6-31G basis using the linear method, with the initial guess being the optimized wave function for  $r_{NN} = 1.5 \text{ \AA}$ . Statistical uncertainties for the individual points are smaller than the symbol size, and the dashed line shows our best JAGP energy for this geometry.

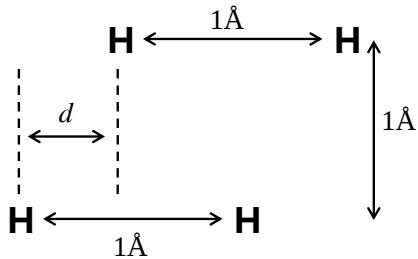


FIG. 4: Schematic of the  $H_4$  distortion, where the geometry is a square when the offset  $d = 0$ .

tion with a Hessian approximated by finite differences among a stored history of energy gradients. This optimization is simple to execute for our wave function, as it requires only the energy and its gradients with respect to the wave function parameters, which may be easily constructed using the derivative ratios of Sec. II E. In Figures 1 and 2, we see that the LM greatly outperforms the L-BFGS algorithm in both lowering the energy and reducing the energy gradient, converging in a small fraction of the number of iterations necessary for L-BFGS. Note that even in the first 50 iterations, during which the length-50 history L-BFGS is equivalent to full BFGS, the LM is still far superior. We also note that, thanks to the size-consistency recovered by the Jastrow factor, the JAGP is an essentially exact description of this system. This accuracy should not be surprising, as the system is constructed of weakly interacting two-electron subsystems, an ideal case for JAGP.

For our second example, we inspect a typical Monte

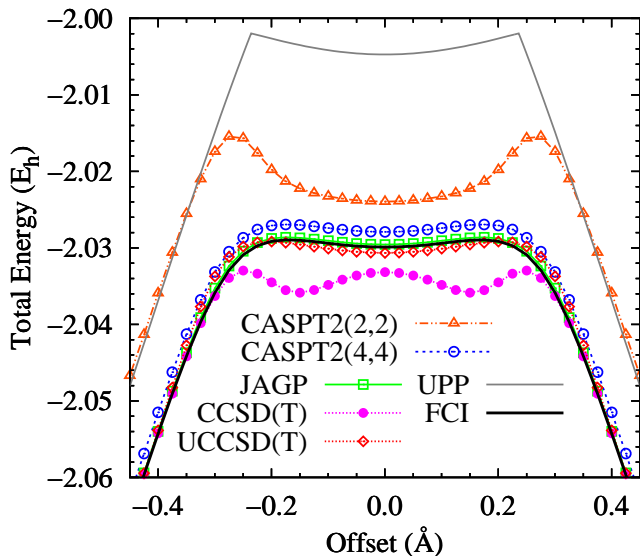


FIG. 5: Total energies of the  $H_4$  distortion of Figure 4 for different offsets  $d$ . The 6-31G basis set was used, and statistical uncertainties for JAGP are smaller than the symbol size.

Carlo optimization for the nitrogen molecule in the 6-31G basis set [38]. Two features of the optimization shown in Figure 3 stand out. First, we see a rapid convergence to the energy minimum, with fewer than ten iterations necessary to get within 1 kcal/mol of the best JAGP energy. Second, we see that as the minimum is approached, the energies of successive updates stop decreasing monotonically, with oscillations observed that are outside the statistical uncertainties of the individual energy points. These oscillations are caused by updates in which the parameters are easily “over-optimized” for a particular random sample in a way that lowers the energy for that sample while raising it for other samples. While we can prevent this over-optimization by taking larger sample sets, such effort is not strictly necessary. Indeed, we will see in the remainder of the results that the minimum energies produced by these somewhat noisy optimizations are already quite accurate, and due to the variational principle we do not have to worry about these oscillations causing us to overshoot the exact energy.

## B. $H_4$ distortion

To demonstrate the JAGP’s ability to handle strong correlations between more than two electrons in a simple and clear example, we have applied it to the four-hydrogen distortion coordinate shown in Figure 4, which deforms a square of hydrogen atoms into a parallelogram. While the strongest correlations in this system arise from the two higher-energy electrons that must navigate the near-degeneracy of the second and third molecular orbitals, significant strong correlations are present for all

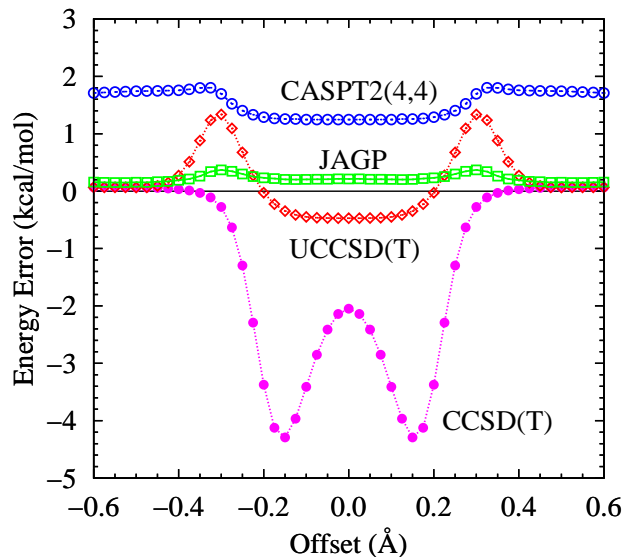


FIG. 6: Energy errors vs FCI for the  $H_4$  distortion of Figure 4 for different offsets  $d$ . The 6-31G basis set was used, and statistical uncertainties for JAGP are smaller than the symbol size.



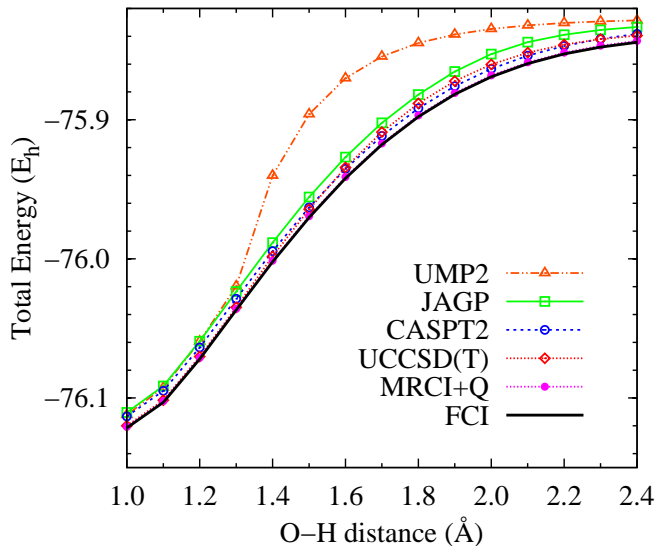


FIG. 7: Total energies for the symmetric stretch of  $\text{H}_2\text{O}$  in the 6-31G basis with a bond angle of  $109.57^\circ$ . Statistical uncertainties for JAGP are smaller than the symbol size.

four electrons, as evidenced by the fact that a (2,2) active space is an insufficient starting point for CASPT2. Indeed, we see in Figure 5 that CASPT2 is only correct when starting with a (4,4) “full valence” active space, and so by the definition that correlation is strong when it cannot be treated perturbatively, we see that all four electrons are strongly correlated.

As one might expect from this active space analysis, the high-level single-reference method CCSD(T) fails qualitatively in this system, predicting unphysical local minima at offsets of  $d = \pm 0.15$  Å. These unphysical minima can be removed by breaking spin symmetry in the Hartree-Fock reference and generalizing to UCCSD(T). However, this approach simply trades one qualitative failure for another, as the UHF determinant is strongly spin contaminated with an unphysical  $\langle S^2 \rangle \approx 1$  for small offsets. Even with this sacrifice, we see in Figure 6 that UCCSD(T) is still not energetically competitive with true multi-reference methods.

In this example we see clearly that the JAGP is capable of treating strong correlation even when more than two electrons are involved, a fundamental step beyond the capabilities of PP. Restricted PP (not shown) fails even to predict an energy plateau, while unrestricted PP (UPP) displays sharp cusps in its potential energy surface. These cusps are caused by the crossing of UPP solutions [8] that represent different valence bond structures. JAGP, on the other hand, is able to create a superposition of these competing valence bond structures, removing the unphysical cusps and producing a good spin eigenstate with  $\langle S^2 \rangle < 0.01$  at all offsets. This feature of JAGP appears to be relatively robust: JAGP predicts pure spin eigenstates in all systems tested, even when spin unrestricted is necessary to produce a qualitatively

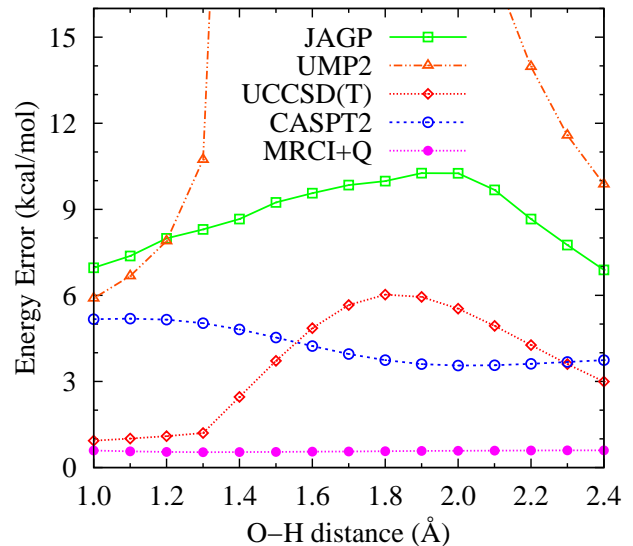


FIG. 8: Energy errors vs FCI for the symmetric stretch of  $\text{H}_2\text{O}$  in the 6-31G basis. Statistical uncertainties for JAGP are smaller than the symbol size.

correct coupled cluster result. In terms of energy error, JAGP is the most accurate method tested in this system in both an absolute sense and in terms of non-parallelity error (NPE), defined as the difference between a method’s largest and smallest deviations from FCI.

### C. $\text{H}_2\text{O}$ stretch

Previously [15] we reported results on the symmetric  $\text{H}_2\text{O}$  stretch in a minimal STO-3G basis, showing that JAGP’s worst error relative to FCI was less than 2 kcal/mol. Here we extend this demonstration to include dynamic correlation, showing results for the symmetric stretch in a 6-31G basis in Figures 7 and 8. Two features are immediately clear. First, JAGP still delivers a qualitatively correct potential energy surface with a 3.4 kcal/mol NPE that is smaller than the 5.1 kcal/mol NPE of UCCSD(T) (restricted CCSD(T) performs extremely poorly and is not shown). Second, absolute errors are significantly larger in 6-31G as compared to STO-3G, topping out around 10 kcal/mol at an OH distance of 2 Å. A third important feature not shown in the figures is that the optimized JAGP wave function is a good spin eigenstate with  $\langle S^2 \rangle$  calculated to be less than 0.01 across the entire stretching coordinate.

Given JAGP’s high accuracy in capturing the strong correlations present in STO-3G, these findings imply that it lacks a full accounting of the details of dynamic correlation. This shortcoming is most obvious near equilibrium, where JAGP is missing 7 kcal/mol of correlation energy even though strong correlations are not present. Clearly, future development of this theory should focus on capturing the remaining dynamic correlation, a point to which

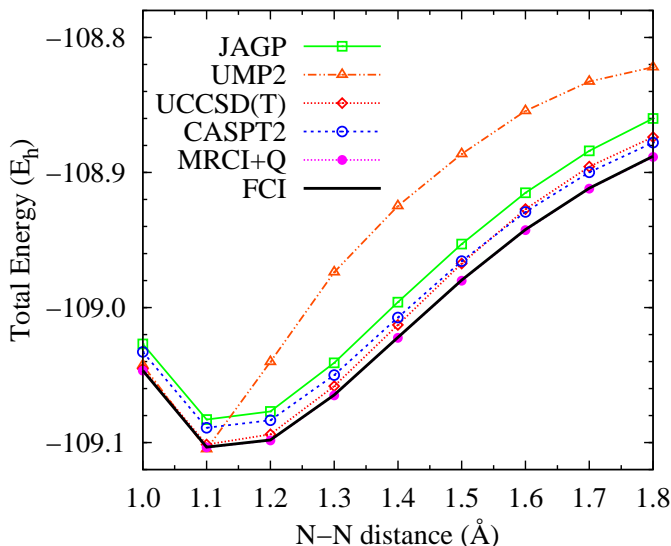


FIG. 9: Total energies for stretched  $N_2$  in the 6-31G basis. Statistical uncertainties for JAGP are smaller than the symbol size.

we will return in the conclusion. Nonetheless, for the  $H_2O$  stretch, the JAGP provides a more accurate potential energy surface than unrestricted single reference methods while avoiding the exponential cost of active space methods.

#### D. $N_2$ stretch

JAGP results for stretching the  $N_2$  triple bond are shown in Figures 9 and 10. As in  $H_2O$ , the NPE is better than that of single reference methods but not as good as that of CASPT2, while absolute errors are relatively large (12 to 17 kcal/mol). Again, the state is a good spin singlet across the entire stretching coordinate.

Although at first glance these results do not seem to provide much insight beyond what was gleaned from  $H_2O$ , it is important to consider that in  $N_2$  the six strongly correlated electrons are all in close proximity to each other, while in  $H_2O$  there is at least some spatial separation into two distinct bonds. We therefore conclude that while the JAGP is ideally suited for describing spatially separated pairs, it is not wholly reliant on such structure and can produce faithful descriptions of the strong correlations of even a close-proximity six-electron problem like  $N_2$ .

#### E. $C_2$ triplet

To test the JAGP’s performance in a non-singlet state, we have applied it to the triplet  $B_{2u}$  state of  $C_2$ , for which stretching coordinate data are shown in Figures 11 and 12. We accessed the triplet state by adding a distant

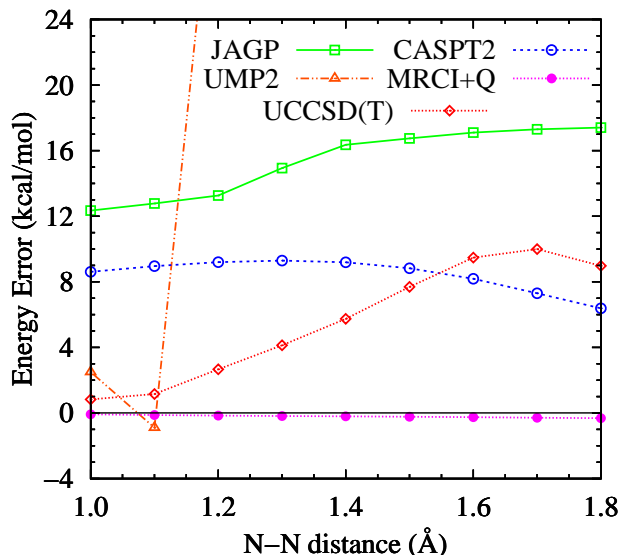


FIG. 10: Energy errors vs FCI for stretched  $N_2$  in the 6-31G basis. Statistical uncertainties for JAGP are smaller than the symbol size.

$H_2$  molecule to the system and applying number projecting Jastrow factors to ensure the net  $S_z$  spin of  $C_2$  was +1 while that of  $H_2$  was -1 (thus circumventing the restriction that an AGP wave function must have equal numbers of  $\alpha$  and  $\beta$  electrons). In our results we have subtracted away the energy of the  $H_2$  triplet. The  $B_{2u}$  representation was enforced by using symmetrized atomic orbitals and allowing the random walk to visit only those configurations with  $B_{2u}$  symmetry. This scheme is essentially another way to perform variation after symmetry and number projection [39] with the added benefit of including Jastrow factors.

We see in the results that all methods have more trouble in  $C_2$  than for  $H_2O$  or  $N_2$ , with JAGP giving a non-parallelity error slightly better than that of ROHF-UCCSD(T) and slightly worse than that of CASPT2. Notably, even MRCI+Q has difficulty in this example, showing a variational violation and an uncharacteristically large non-parallelity error. Overall, we see that JAGP’s performance for a triplet state is similar to that for singlets, delivering a good spin eigenstate ( $\langle S^2 \rangle = 2$ ) and an accuracy approaching that of CASPT2.

#### F. Ethene

As a final example, we have used the JAGP wave function to predict barrier heights for the unassisted gas phase insertion of  $H_2$  into ethene’s double bond. Using CASSCF with a (4,4) active space in the 6-31G basis, we have located the two saddle point structures shown in Figures 13 and 14 using the quadratic steepest descent (QSD) method [40] as implemented in MOLPRO (coordinates can be found in the Appendix). The first

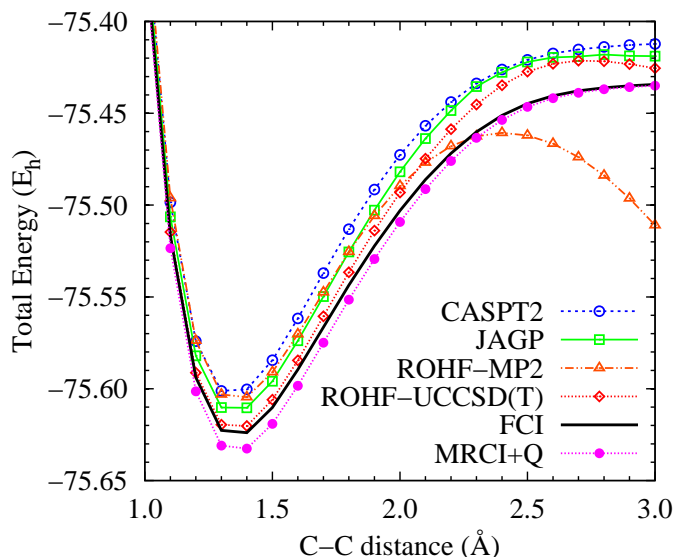


FIG. 11: Total energies for the triplet  $B_{2u}$  state of  $C_2$  in the 6-31G basis. Statistical uncertainties for JAGP are smaller than the symbol size.

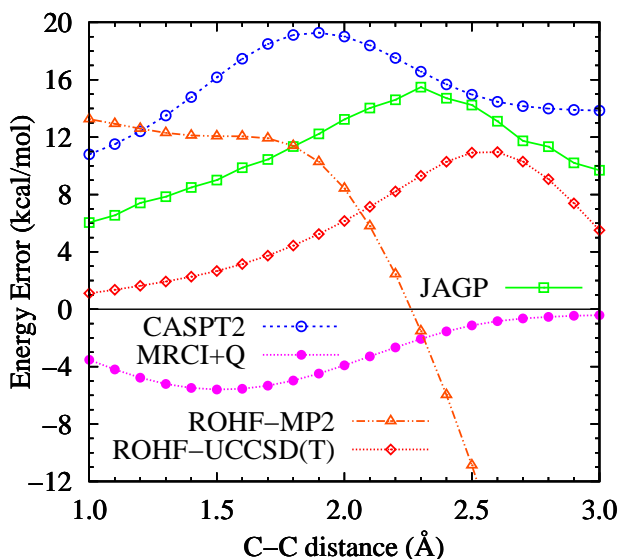


FIG. 12: Energy errors vs FCI for the triplet  $B_{2u}$  state of  $C_2$  in the 6-31G basis. Statistical uncertainties for JAGP are smaller than the symbol size.

structure has  $C_s$  symmetry, is single-reference in nature, and has been found previously using density functional theory [41]. The second structure has  $C_{2v}$  symmetry, is multi-reference in nature, and does not appear to have been reported previously.

These saddle points correspond to transition states for two different mechanisms of the unassisted gas phase hydrogenation reaction. We have verified that they are indeed transition states by computing intrinsic reaction coordinates (IRCs) towards both products and reactants starting from these structures (again via the

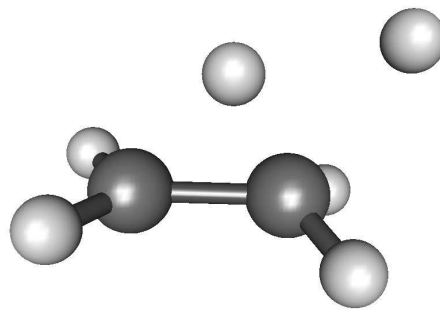


FIG. 13: Transition state for the  $C_s$  mechanism.

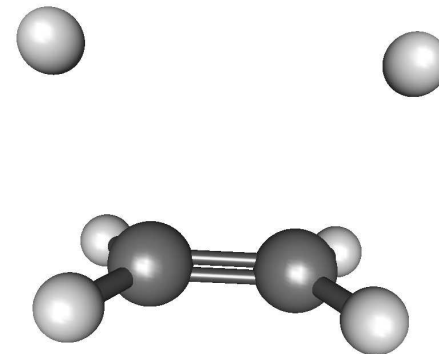


FIG. 14: Transition state for the  $C_{2v}$  mechanism.

QSD method). In both cases, these structures are the maximum-energy points for their respective IRCs. The mechanism for the  $C_s$  transition state involves “sliding”  $H_2$  in from one side, which has the advantage of not having to fully break the  $H_2$  bond until late in the reaction coordinate when significant C-H bonding has already begun. In the  $C_{2v}$  mechanism, on the other hand, the  $H_2$  bond is broken already at the transition structure, which at first glance makes this mechanism appear uncompetitive.

What is especially interesting about the  $C_{2v}$  structure is that despite its multi-reference nature (the CASSCF active natural orbital occupations are 1.9, 1.2, 0.8, and 0.1), and the fact that the  $H_2$  bond is already broken, its barrier height is essentially the same as that of the single-reference  $C_s$  structure. Indeed, JAGP predicts the  $C_s$  and  $C_{2v}$  barriers to be 136 and 135 kcal/mol, respectively, as shown in Table II. This nearly equal-height prediction is corroborated by the benchmark MRCI+Q and by UCCSD(T), but *not* by CCSD(T), MP2, UMP2, B3LYP, or UB3LYP, which predict to different degrees a significant difference between the two barriers. Thus at temperatures high enough for this unassisted reaction to proceed, high-level methods predict that two mechanistic channels will be in essentially equal competition, while other methods (especially MP2, UB3LYP, and B3LYP) erroneously predict that one pathway will be significantly favored.

TABLE II: Barrier heights (kcal/mol) for ethene hydrogenation mechanisms at the 6-31G CASSCF(4,4) geometries. JAGP statistical uncertainties are less than 1 kcal/mol.

Method	$C_s$	$C_{2v}$
B3LYP	130.0	170.3
UB3LYP	130.0	146.4
MP2	139.8	177.5
UMP2	144.4	139.9
CCSD(T)	131.0	125.5
UCCSD(T)	132.8	134.6
MRCI+Q	130.8	132.5
JAGP	135.9	135.2

#### IV. CONCLUSIONS

This report has detailed efficient algorithms for evaluating and optimizing the energy of the Jastrow antisymmetric geminal power (JAGP) wave function in Hilbert space. This ansatz represents an alternative approach for approximating the electronic structure of molecules and materials that relies on neither the independent particle approximation nor the active space framework. Instead, the basic assumption is that the strongest correlations between electrons can be broken down in a pairwise fashion, with the overall wave function constructed as a superposition of valence bonding structures built in turn from products of local two-electron functions. The JAGP attempts to encode this structure by placing all electrons in a single “molecular” geminal that holds an arbitrary linear combination of the non-orthogonal local geminal building blocks. Raising this geminal to the appropriate power produces a superposition of geminal products, from which the Jastrow factor selects the desired resonating valence bond structures by projecting out terms with undesirable local particle number distributions.

Our results demonstrate that for a variety of strongly correlated examples, JAGP delivers good spin eigenstates with potential energy surfaces superior in quality to those of the most accurate single-reference methods and approaching the quality of CASPT2 results. These examples include singlet and triplet multi-bond dissociations as well as a reaction mechanism involving a novel multi-reference transition state. Furthermore, this accuracy is coupled with good formal properties: the JAGP is variational, size consistent, and can be optimized in polynomial time for a cost that scales as the fifth power of the system size.

The most pressing question that remains to be answered for JAGP is whether its ability to describe dynamic correlation can be improved. One strategy is to use JAGP as a guiding function in fixed-node projector Monte Carlo [42], which is the Hilbert space ana-

logue of fixed-node diffusion Monte Carlo (DMC) [43] and should be capable of capturing the remaining dynamic correlation. Alternatively, if the local-particle-number-projecting qualities of the Hilbert space Jastrow factor can be transported into real space, then a combination of traditional cusp-providing Jastrow factors [43] and real space DMC would likely serve to provide the missing dynamic correlation. Finally, even within the VMC framework, there is still scope to improve the JAGP by generalizing to a Pfaffian geminal [44, 45] and by optimizing the local orbital basis in which the Jastrow factor is defined. Research in these exciting directions is underway.

#### V. ACKNOWLEDGMENTS

We thank Martin Head-Gordon for many insightful discussions and for computational resources. We thank the Miller Institute for Basic Research in Science for funding.

#### Appendix A: Transition States

TABLE III: Geometry, in Angstroms, of the CASSCF(4,4) 6-31G  $C_s$  transition state of the unassisted gas phase ethene hydrogenation reaction.

C	0.0000000000	0.0087063743	-0.7990056481
C	0.0000000000	-0.1355804403	0.6628393017
H	0.0000000000	1.0510492173	0.2326305655
H	0.0000000000	1.2421143685	1.8005988762
H	0.9012117308	-0.4823664902	1.1231614214
H	-0.9012117308	-0.4823664902	1.1231614214
H	-0.9255826314	0.0917247367	-1.3284709121
H	0.9255826314	0.0917247367	-1.3284709121

TABLE IV: Geometry, in Angstroms, of the CASSCF(4,4) 6-31G  $C_{2v}$  transition state of the unassisted gas phase ethene hydrogenation reaction.

C	-0.6834781870	0.0000000000	-0.1205362034
C	0.6834781870	0.0000000000	-0.1205362034
H	-1.5774417549	0.0000000000	1.8385459217
H	1.5774417549	0.0000000000	1.8385459217
H	1.2414310806	0.9128454494	-0.2010951235
H	1.2414310806	-0.9128454494	-0.2010951235
H	-1.2414310806	-0.9128454494	-0.2010951235
H	-1.2414310806	0.9128454494	-0.2010951235

- 
- [1] R. G. Parr and W. Yang, *Density-functional theory of atoms and molecules*, Oxford University Press, New York, 1989.
- [2] A. Szabo and N. S. Ostlund, *Modern Quantum Chemistry: Introduction to Advanced Electronic Structure Theory*, Dover Publications, Mineola, N.Y., 1996.
- [3] R. J. Bartlett and M. Musiał, *Rev. Mod. Phys.* **79**, 291 (2007).
- [4] T. Helgaker, P. Jørgensen, and J. Olsen, *Molecular Electronic Structure Theory*, John Wiley & Sons, Ltd., West Sussex, England, 2000.
- [5] A. C. Hurley, J. Lennard-Jones, and J. A. Pople, *Proc. R. Soc. London, Ser. A* **220**, 446 (1953).
- [6] P. A. Limacher et al., *J. Chem. Theory Comput.* **9**, 1394 (2013).
- [7] W. Kutzelnigg and D. Mukherjee, *J. Chem. Phys.* **110**, 2800 (1999).
- [8] J. A. Parkhill, K. Lawler, and M. Head-Gordon, *J. Chem. Phys.* **130**, 084101 (2009).
- [9] P. J. Hay, T. H. Dunning Jr., and W. A. Goddard III, *J. Chem. Phys.* **62**, 3912 (1975).
- [10] P. R. Surján, Ágnes Szabados, P. Jeszenszki, and T. Zoboki, *J. Math. Chem.* **50**, 534 (2012).
- [11] J. A. Parkhill and M. Head-Gordon, *J. Chem. Phys.* **133**, 024103 (2010).
- [12] D. W. Small and M. Head-Gordon, *J. Chem. Phys.* **130**, 084103 (2009).
- [13] P. Cassam-Chenaï and F. Patras, *J. Math. Phys.* **44**, 4884 (2003).
- [14] P. Cassam-Chenaï, *J. Chem. Phys.* **124**, 194109 (2006).
- [15] E. Neuscammann, *Phys. Rev. Lett.* **109**, 203001 (2012).
- [16] M. Casula and S. Sorella, *J. Chem. Phys.* **119**, 6500 (2003).
- [17] M. Casula, C. Attaccalite, and S. Sorella, *J. Chem. Phys.* **121**, 024512 (2004).
- [18] S. Sorella, M. Casula, and D. Rocca, *J. Chem. Phys.* **127**, 014105 (2007).
- [19] M. Marchi, S. Azadi, M. Casula, and S. Sorella, *J. Chem. Phys.* **131**, 154116 (2009).
- [20] M. P. Nightingale and C. J. Umrigar, editors, *Quantum Monte Carlo Methods in Physics and Chemistry*, NATO ASI Ser. C 525, Kluwer, Dordrecht, 1999.
- [21] J. Bouchaud, A. Georges, and C. Lhuillier, *J. Phys. (France)* **49**, 553 (1988).
- [22] M. Brookes, The matrix reference manual [online], 2011, [www.ee.imperial.ac.uk/hp/staff/dmb/matrix/intro.html](http://www.ee.imperial.ac.uk/hp/staff/dmb/matrix/intro.html).
- [23] A. Griewank and A. Walther, *Evaluating Derivatives, Principles and Techniques of Algorithmic Differentiation, Second Edition*, Society for Industrial and Applied Mathematics, Philadelphia, 2008.
- [24] C. J. Umrigar, J. Toulouse, C. Filippi, S. Sorella, and R. G. Hennig, *Phys. Rev. Lett.* **98**, 110201 (2007).
- [25] J. Toulouse and C. J. Umrigar, *J. Chem. Phys.* **128**, 174101 (2008).
- [26] T. D. Crawford et al., *J. Comput. Chem.* **28**, 1610 (2007).
- [27] P. Knowles and N. Handy, *Chem. Phys. Lett.* **111**, 315 (1984).
- [28] P. Knowles and N. Handy, *Comp. Phys. Commun.* **54**, 75 (1989).
- [29] H.-J. Werner, *Mol. Phys.* **89**, 645 (1996).
- [30] H.-J. Werner and P. J. Knowles, *J. Chem. Phys.* **89**, 5803 (1988).
- [31] P. J. Knowles and H.-J. Werner, *Chem. Phys. Lett.* **145**, 514 (1988).
- [32] H.-J. Werner et al., MOLPRO, version 2012.1, a package of ab initio programs, see <http://www.molpro.net>.
- [33] G. J. O. Beran, B. Austin, A. Sodt, and M. Head-Gordon, *J. Phys. Chem. A* **109**, 9183 (2005).
- [34] A. D. Becke, *J. Chem. Phys.* **98**, 5648 (1993).
- [35] A. Krylov and P. Gill, *WIREs Comput. Mol. Sci.* **3**, 317 (2013).
- [36] W. J. Hehre, R. F. Stewart, and J. A. Pople, *J. Chem. Phys.* **51**, 2657 (1969).
- [37] J. Nocedal, *Math. Comp.* **35**, 773 (1980).
- [38] W. J. Hehre, R. Ditchfield, and J. A. Pople, *J. Chem. Phys.* **56**, 2257 (1972).
- [39] C. A. Jiménez-Hoyos, T. M. Henderson, T. Tsuchimochi, and G. E. Scuseria, *J. Chem. Phys.* **136**, 164109 (2012).
- [40] J.-Q. Sun and K. Ruedenberg, *J. Chem. Phys.* **101**, 2157 (1994).
- [41] S. Senger and L. Radom, *J. Phys. Chem. A* **104**, 7375 (2000).
- [42] D. F. B. ten Haaf, H. J. M. van Bemmelen, J. M. J. van Leeuwen, W. van Saarloos, and D. M. Ceperley, *Phys. Rev. B* **51**, 13039 (1995).
- [43] W. M. C. Foulkes, L. Mitas, R. J. Needs, and G. Rajagopal, *Rev. Mod. Phys.* **73**, 33 (2001).
- [44] M. Bajdich, L. Mitas, G. Drobný, L. K. Wagner, and K. E. Schmidt, *Phys. Rev. Lett.* **96**, 130201 (2006).
- [45] M. Bajdich, L. Mitas, L. K. Wagner, and K. E. Schmidt, *Phys. Rev. B* **77**, 115112 (2008).